The Sixth International Supercritical $CO_2$ Power Cycles Symposium
March 27–29, 2018, Pittsburgh, Pennsylvania

# Partial Load Characteristics of the Supercritical $CO_2$ Gas Turbine System for the Solar Thermal Power System with the Na-Al-$CO_2$ Heat Exchanger

Yasushi Muto
Research Associate
Tokyo Institute of Technology
O-okayama, Meguro-ku, Tokyo, Japan
muto@nr.titech.ac.jp

Noriyuki Watanabe
Assistant Professor
Nagoya University
Furoh-cho, Chigusa-ku, Nagoya, Japan
tobenori_ctb13_fzr@yahoo.co.jp

Masanori Aritomi
Research Associate
Tokyo Institute of Technology
O-okayama, Meguro-ku, Tokyo, Japan
maritomimasa@gmail.com

Takao Ishizuka
Research Associate
Tokyo Institute of Technology
O-okayama, Meguro-ku, Tokyo, Japan
takao.i@nr.titech.ac.jp

## ABSTRACT

For a concentrated solar power system, supercritical $CO_2$ gas turbines are a particularly promising application. However, they cannot be applied effectively in existing systems using molten salt because of the maximum temperature limit of the molten salt: 600°C. A newly developed system includes a Na-cooled receiver, aluminum heat storage, and a supercritical $CO_2$ gas turbine. This new system uses both the latent heat and the sensible heat of aluminum. In this case, the aluminum temperature decreases considerably at night. However, in the S-$CO_2$ GT cycle, outlet flow of the recuperator 2 high-pressure side joins the bypass compressor outlet flow to improve the recuperator effectiveness. The possibility exists of inducing a severe partial load operation problem. Partial load operation analyses were conducted by preparing a cycle calculation code combined with recuperator performance calculation sub-routines. Time histories of the $CO_2$ temperature, pressure, heater heat load, and generator power are calculated. Thermal efficiency calculated is 26.9%. Regarding the end temperature difference problem, the minimum value is less than 2°C, which is too small for the stable operation. More comprehensive studies including partial load performance of the turbomachinery should be conducted.

## INTRODUCTION

An earlier paper (Muto, 2016) presented at the Fifth International Supercritical $CO_2$ Power Cycles Symposium described the application of two $CO_2$ GT cycles, i.e., 20 MPa supercritical $CO_2$ GT cycle and 10 MPa Brayton $CO_2$ GT cycle, to a 100 MW thermal solar thermal power plant. They were compared in terms of their design features. The solar power plant has a tower top receiver cooled by liquid sodium (Na). The main solar thermal energy transported to Na is transferred via aluminum to $CO_2$. The residual thermal energy is used to heat the aluminum in the heat exchanger. In the 20 MPa supercritical $CO_2$ gas turbine (S-$CO_2$-GT) cycle, $CO_2$ temperatures were 650°C and 467°C, respectively, at the turbine inlet and the heat exchanger inlet. The maximum achievable value of the cycle thermal efficiency was found to be 48.9%.

The existing concentrated solar power plant uses the molten salt (a mixture of $KNO_3$ and $NaNO_3$) and a steam turbine. By substituting the S-$CO_2$-GT for the steam turbine, higher efficiency can be achieved. However, at the upper limit of the molten salt (600°C), the maximum possible turbine inlet temperature is 550°C. Since the respective values of cycle thermal efficiency are 48.9% and 44.9% at 650°C and at 550°C, the S-$CO_2$-GT cannot be applied effectively. As new heat transfer and heat storage materials, a combination of Na and Al can be considered. The Na is an excellent heat transfer fluid. Better receiver design can be expected. The aluminum has the large heat of fusion of 397 kJ/kg. Its melting temperature is 660.3°C. The large latent heat is useful for the S-$CO_2$-GT cycle at 650°C. In addition, the specific heat of Al of 0.897 kJ/kg/K is large. Therefore a high-efficiency solar thermal plant could be realized if Na were used for the heat transfer fluid for the receiver, Al for the heat storage material, and S-$CO_2$ for the turbine.

In the new solar thermal power generation system presented above, the aluminum is solid in the morning. At sunrise, the aluminum temperature increases by the solar radiation, reaching a melting value of 660°C in the afternoon. The aluminum melting begins from the top and proceeds gradually downward. The melting area expands until saturation near the time of sunset. About 30% of the top and hot area of Al will be melted. After sunset, solidification of the melted aluminum begins. The heat of fusion is emitted, keeping the temperature of the aluminum roughly constant. In the evening, the heat source for the S-$CO_2$-GT cycle switches from latent heat to sensible heat. The aluminum temperature continues to decrease through the night until the next sunrise. The S-$CO_2$-GT must be controlled to adjust the $CO_2$ receiving thermal energy to the power demand. The closed cycle gas turbine generally uses an inventory control, i.e., a pressure level control because the cycle thermal efficiency value is roughly constant in cases of an ideal gas turbine such as a helium turbine. However, some difficulties arise in cases of the supercritical $CO_2$ cycle gas turbine. First, the compression power increases with the pressure reduction and markedly reduces power generation. Second, the rated balances of heat capacity between the high-temperature side and the low-temperature side of the two recuperators are lost. This imbalance reduces the recuperator temperature effectiveness. In an extreme case, a value of the end temperature difference becomes very small and the stable operation will be hindered. In addition, the Al temperature decreases during the night with the utilization of sensible heat. The turbine inlet temperature must be lower than the aluminum temperature, which imposes an additional restriction to the S-$CO_2$-GT cycle.

As described herein, partial load characteristics of the supercritical $CO_2$ cycle for the solar thermal power application with Na-Al-$CO_2$ heat exchanger are calculated under simplified quasi-steady assumptions. To adjust the $CO_2$ power generated to the power demand during day and night, the pressure and the necessary temperature values are estimated. Results clarified the feasibility of inventory control.

## THE SOLAR POWER SYSTEM COMPRISES A Na-COOLED RECEIVER, Na-Al-$CO_2$ HEAT EXCHANGER AND S-$CO_2$-GT

The system concept is presented in Fig. 1. The solar energy collecting system, based on an existing concentrated solar power system, has numerous heliostats and a receiver tower. The reference system described in the literature (Hasuike, 2006) has solar capacity of 125 MW. The receiver tower is located at the center of the 800 m diameter circular field. The upper focus is 103 m high.

The receiver is a cylindrical tower provided with an annular channel for the Na coolant flow. The diameter, the effective height, and Na channel width are, respectively, 9.1 m, 16.6 m and 20 mm. The Na enters the receiver at 600°C and 0.16 MPa and flows out at 700°C and 0.15 MPa. The pressure drop is less than 0.01 MPa. The Na pumping power is 10.8 kW. Solar energy of 12.5 MW is reflected and lost at the outer surface of the receiver. The radiation loss and the convection loss are, respectively, 25.24 MW and 3.32 MW. The net solar energy into the Na is 83.94 MW. The receiver efficiency becomes 67.15%, which is defined as the ratio of 83.94 MW to 125 MW.

The Na-Al-$CO_2$ heat exchanger consists of Na heat transfer U-tubes, $CO_2$ heat transfer U-tubes, an inner Al filled vessel and an airtight outside vessel. The Na and $CO_2$ heat transfer tubes are installed horizontally, alternately arranged. The rectangular outside vessel has width, height and depth that are, respectively, 11.6 m, 2.22 m and 57.8 m. Vertical pitch and horizontal pitch for the heat transfer tubes are, respectively, 0.3025 m and 0.26 m. The dimensions and materials are presented below.

Na heat transfer tubes
Outer diameter = 60.5 mm, Inner diameter = 53.5 mm, 304SS

$CO_2$ heat transfer tubes
Outer diameter = 60.5 mm, Inner diameter = 34.7 mm, 304SS

The heat transfer data for the Na-Al-$CO_2$ heat exchanger are shown in Table 1. Half of the heat transferred to Al from Na is transported to the $CO_2$ loop. The residual half is once stored in Al as the latent heat. These are presented in Fig. 2.

The aluminum weight is 3364 ton whose 30% are planned to be melted. Capacities of the latent heat and sensible heat are $0.385 \times 10^6$ MJ and $1.05 \times 10^6$ MJ, respectively. The total heat capacity is $1.44 \times 10^6$

MJ (399 MWhr).

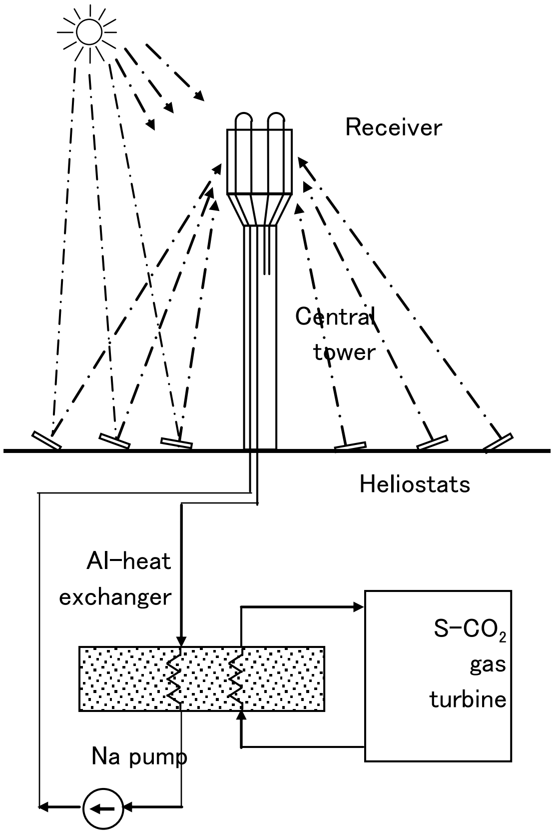


**Fig. 1. Solar thermal power generation system with Na-cooled receiver, Al heat exchanger and $CO_2$ gas turbine.**

Table 1 Heat transfer data of the Na-Al-$CO_2$ heat exchanger at the design condition

| Items | | High-temperature fluid (Na) | Low-temperature fluid ($CO_2$) |
|---|---|---|---|
| Flow rate | kg/s | 660.97 | 177.60 |
| Inlet temperature | °C | 700 | 460 |
| Outlet temperature | °C | 600 | 650 |
| Inlet pressure | MPa | 0.15 | 20.20 |
| Outlet pressure | MPa | 0.108 | 20.17 |
| Heat transferred | MW | 83.94 | 41.97 |
| Pumping power needed | kW | 47.8 | 63.2 |

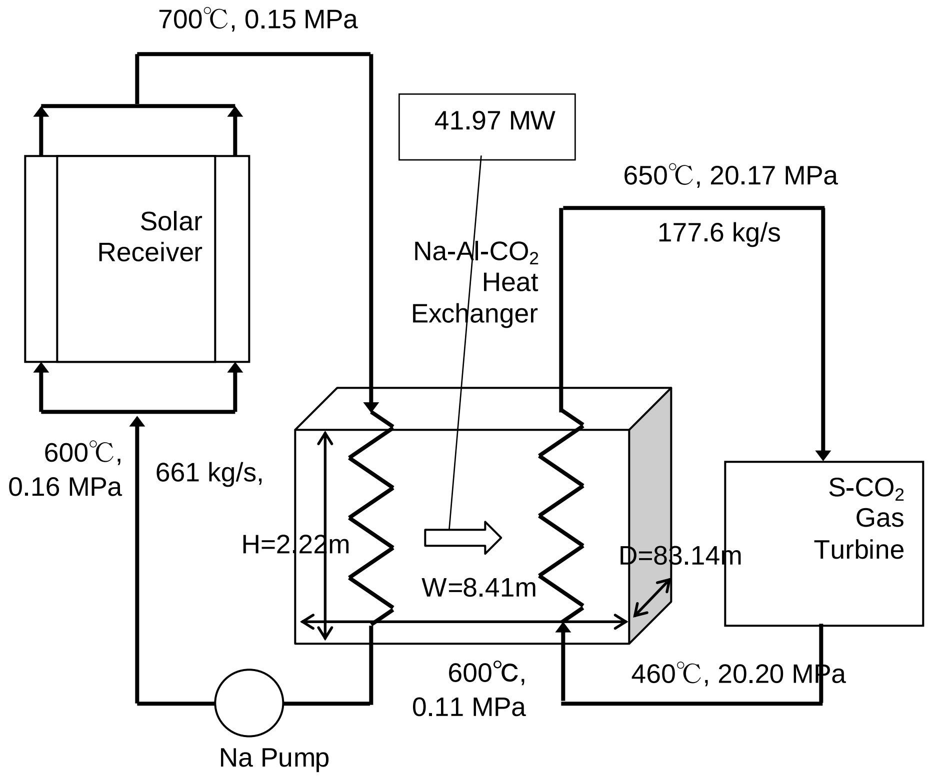


**Fig. 2. Solar thermal power generation system with a Na-cooled receiver, Al heat exchanger, and $CO_2$ gas turbine.**

An intercooled cycle is used because the cycle thermal efficiency is 2% higher than that of the non-intercooled cycle at 650°C for the S-$CO_2$-GT cycle (Muto, 2013). This typical supercritical $CO_2$ cycle flow scheme has a bypass circuit and a bypass compressor. Assumed cycle design data are shown below.

| | |
|---|---|
| Turbine pressure ratio | 2.95 |
| Low-pressure compressor pressure ratio | 1.26 |
| Turbine inlet temperature | 650°C |
| Turbine inlet pressure | 20 MPa |
| Low- and high-pressure compressor inlet temperature | 35°C |
| Heater heat load | 41.97 MW |
| Component pressure ratio | |
| Heater 1.0%, Precooler 1.0%, Intercooler 0.8% | |
| Recuperator high-temperature side 1.2%, Recuperator low-temperature side 0.4%, | |
| Turbine adiabatic efficiency | 92% |
| Compressor adiabatic efficiency | 88% |
| Generator efficiency | 98% |
| Average temperature effectiveness of recuperators | 89% |

Sometimes, the temperature difference between hot and cold ends of the recuperator is extremely small, making the recuperator operation difficult. To avoid this undesirable small temperature difference, moderate average recuperator temperature effectiveness of 89% is used. The cycle design results are depicted in Fig. 3.

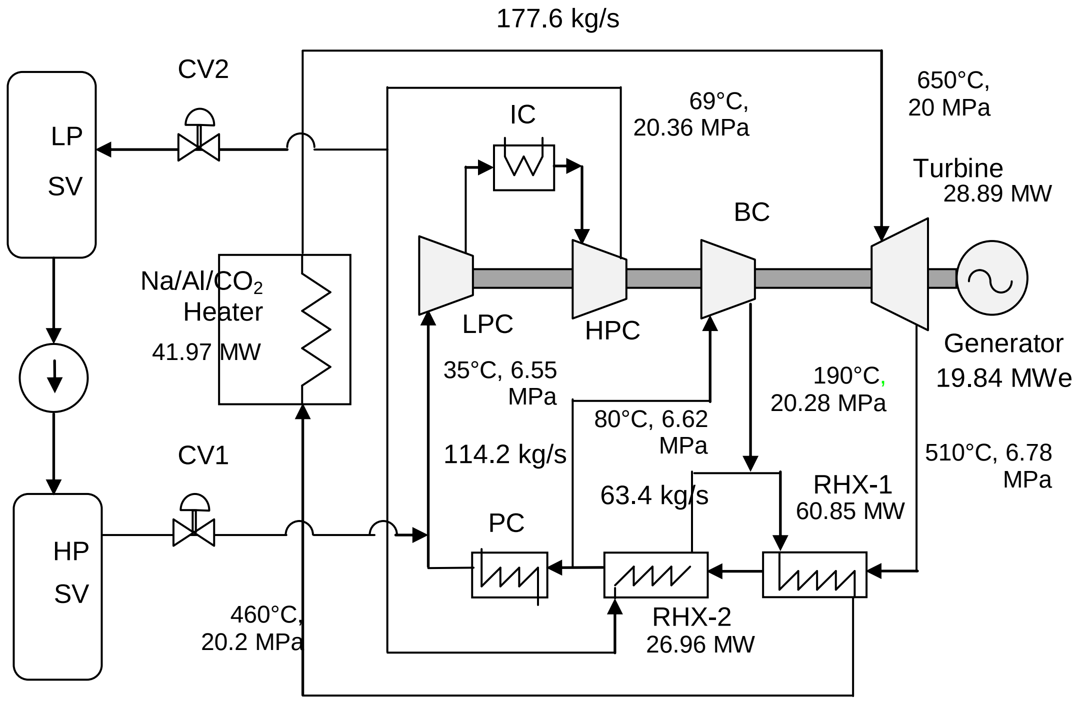


**Fig. 3. Design data for the supercritical $CO_2$ gas turbine cycle.**

Regarding the recuperators, a printed circuit heat exchanger (PCHE) type provided with S-fin portrayed in Fig. 4 (Muto, 2014) is used. The design conditions and results of the design calculations for the recuperators RHX-1 and RHX-2 are shown, respectively, in Table 2 and Table 3.

Table 2 Design conditions of the recuperator modules

| Recuperators | | | RHX-1 | RHX-2 |
|---|---|---|---|---|
| Recuperator average temperature effectiveness | | % | 89 | 89 |
| Number of modules | | | 5 | 5 |
| Heat load | | MW/module | 12.17 | 5.39 |
| High-temperature side | Flow rate | kg/s | 35.52 | 35.52 |
| | Inlet temperature | °C | 509.9 | 210.7 |
| | Inlet pressure | MPa | 6.780 | 6.698 |
| Low-temperature | Flow rate | kg/s | 35.52 | 22.84 |

| | | | |
|---|---|---|---|
| side | Inlet temperature °C | 190.3 | 69.0 |
| | Inlet pressure MPa | 20.283 | 20.365 |

Table 3 Results of the recuperator module design

| Recuperators | | RHX-1 | RHX-2 |
|---|---|---|---|
| Module width m | | 0.26 | 0.26 |
| Module length m | | 1.0 | 1.0 |
| Module height m | | 4.24 | 3.65 |
| Module weight ton | | 7.90 | 6.80 |
| Heat transfer capacity MW/ module | | 12.19 | 5.42 |
| Pressure loss | High temperature side kPa | 50.3 | 38.8 |
| | Low temperature side kPa | 55.1 | 15.4 |
| Effective heat transfer area | High temperature side $m^2$ | 413.7 | 354.6 |
| | Low temperature side $m^2$ | 206.8 | 177.3 |
| Overall heat transfer coefficient based on high temperature side area $J/m^2/K/s$ | | 909 | 1049 |

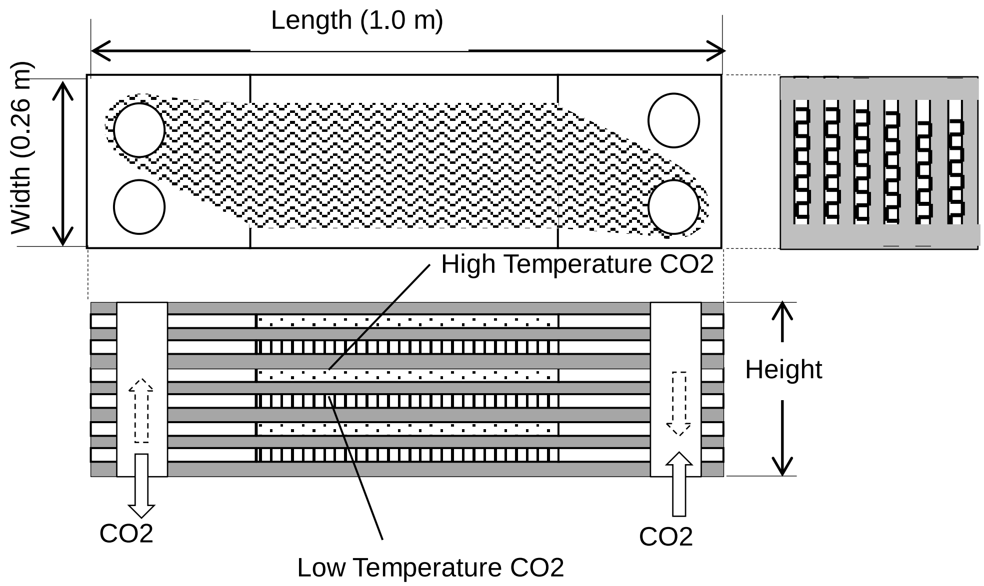


**Fig. 4. Structure and dimensions of the PCHE module.**

## PARTIAL LOAD CHARACTERISTICS OF THE S-$CO_2$ GT SYSTEM FOR THE SOLAR POWER PLANT

The system should be controllable to satisfy power demand. In this solar power plant, the so-called “inventory control” or “pressure level control” is used. This control method is typically used in the closed gas turbine cycle. In this method, control valves CV1 and CV2 depicted in Fig. 3 are operated. To increase power, high-pressure $CO_2$ is charged into the system by opening CV1. To decrease power, the $CO_2$ inventory in the system is discharged to the low-pressure storage vessel by opening CV2.

A partial load cycle calculation code was prepared to assess the S-$CO_2$ GT system status. This code provides the subroutines used to calculate the performance of the recuperators RHX1 and RHX2. The partial load calculations rely upon the following assumptions.

1) The generator keeps the rotational speed constant to meet the grid frequency.
2) In this condition, the pressure ratios of the turbine and the compressors should not be varied. They should be operated within the rated values.
3) It is assumed that the bypass flow ratio is held constant.
4) Pressure loss ratios of the components are assumed not to vary.
5) Inlet temperatures of the low-pressure compressor and the high-pressure compressor are assumed to be kept constant by regulation of the pre-cooler flow rate.
6) The inlet temperature of the RHX-1 high-pressure side is calculated as a mixture of thermal energy of the RHX-2 high-pressure side outlet gas and that of the bypass compressor outlet gas.

Constant input data used for calculations are presented below.

1) Turbine pressure ratio (2.95), low-pressure compressor pressure ratio (1.26)
2) Low-pressure compressor inlet temperature (35°C), high-pressure compressor inlet temperature (35°C)
3) Component pressure ratios, which are the same values as those used for the design
4) Turbine adiabatic efficiency (92%), compressor adiabatic efficiency (88%), generator efficiency (98%)
5) Design turbine flow rate (166.72 kg/s)
6) Design bypass flow ratio (0.357), which is the ratio of the bypass flow rate versus turbine flow rate
7) Design turbine inlet temperature (650°C), Design turbine inlet pressure (20 MPa)
8) Design turbine inlet $CO_2$ density (110 kg/m$^3$)
9) Recuperator dimensions

Parametric input data are values of the turbine inlet pressure and the turbine inlet temperature.

Although the partial load behavior is a transient phenomenon, the transient speed of the state is slow. Therefore, it is possible to conduct calculations as a quasi-static phenomenon. Then, the calculations have been conducted based on steady state.

To begin the time historical calculations, it is convenient to start from the sunset time, i.e., 4:30 p.m., when the aluminum temperature reaches its maximum value, and later time points, when the aluminum temperature is kept roughly constant at the maximum temperature. The following power demands are assumed, where the value at night are determined to be consistent with heat storage capacity. Here, the daytime is assumed 9 hours and then, the night time is 15 hours. 50% of the total energy input in the daytime is assumed to be stored for the power generation at night based on the reference (Dunn, 2012).

From 4:30 p.m. to 8:00 p.m.: 90% of full power

From 8:00 p.m. to 10:00 p.m.: 80% of full power

From 10:00 p.m. to 6:00 a.m.: 38% of full power

From   6:00 a.m. to 7.30 a.m.: 80% of full power

From   7:30 a.m. to 4:30 p.m.: full power

At 4:30 p.m., the $CO_2$ turbine inlet temperature is 650°C. The pressure is slightly lower than 20 MPa to adjust to the 90% power demand. All heat is supplied by the heat of fusion of aluminum until 7:15 p.m. This duration is calculated based on the latent heat capacity.

Subsequently, thermal energy is supplied by the sensible heat of aluminum: the aluminum temperature decreases continuously. At 8:00 p.m., the pressure is reduced further. The value of pressure is determined to adjust the power generated to the power demand planned. After 10:00 p.m., the energy demand is extremely low. The pressure must decrease markedly to 9.1 MPa. The aluminum temperature decreases gradually. The turbine inlet $CO_2$ temperature decreases to 433.9°C at 6:00 a.m. At 6:00 a.m., the power demand increases sharply and the pressure should be raised to 19.7 MPa because no solar energy is being supplied yet.

At 7:30 a.m., the turbine inlet $CO_2$ temperature reaches the minimum value of 370.8°C. Subsequently, the temperature is raised continuously by the supplied solar energy. Before 2:30 p.m., the aluminum temperature achieves the 660.3°C melting point: fusion begins. From that time through 4:30 p.m., the fusion energy is stored in the aluminum.

Temporal changes of both the $CO_2$ pressure and the temperature are presented in Fig. 5. Temporal changes of the heater thermal load, the generator power, and the cycle thermal efficiency are depicted in Fig. 6.

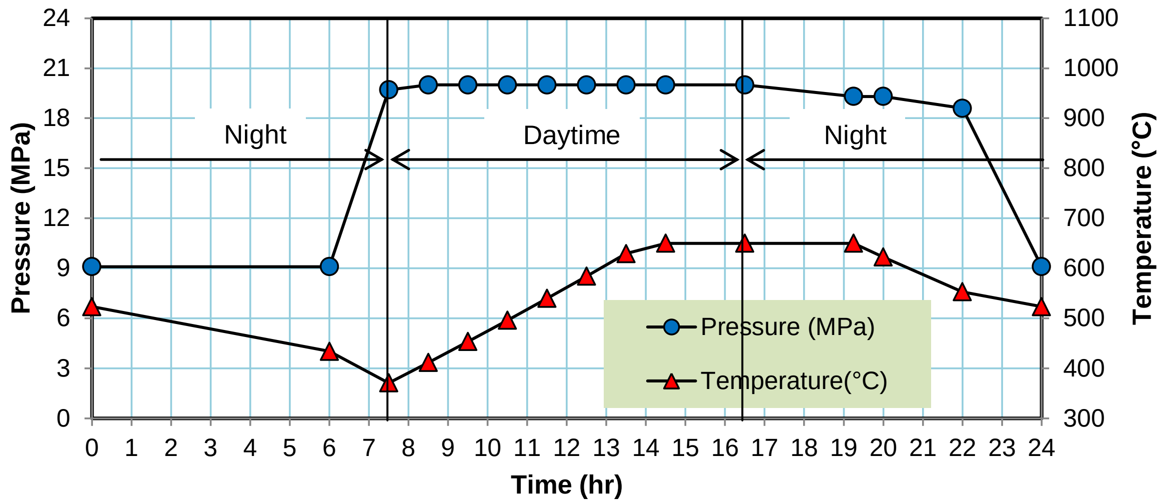


**Fig. 5. Time histories of the turbine inlet pressure and the turbine inlet temperature for the partial load operation.**

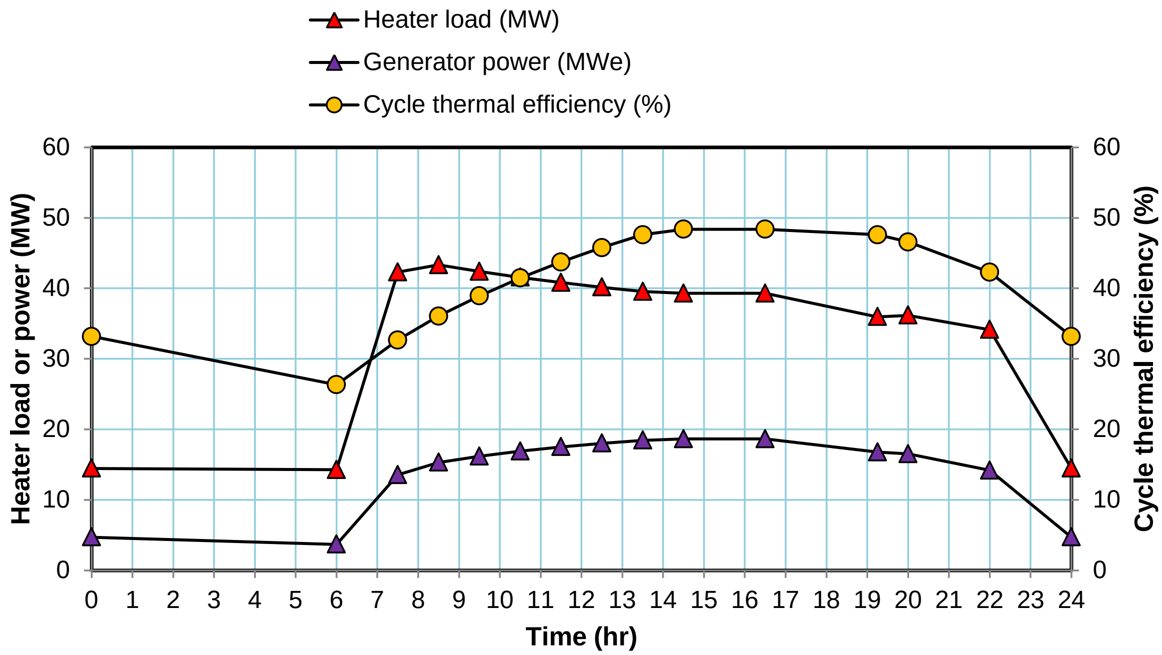


**Fig. 6. Time histories of the heater load, the generator power and the cycle thermal efficiency for the partial load operation.**

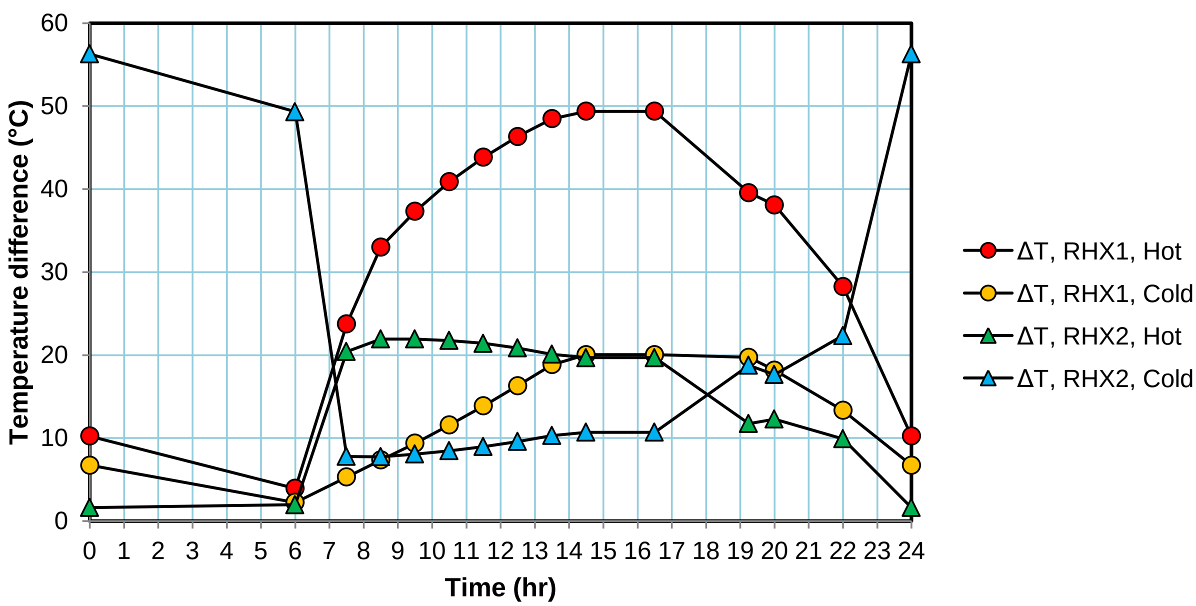


**Fig. 7. Histories of end temperature differences of the recuperators for partial load operation.**

During the partial load operation of S-$CO_2$ GT cycle, undesirably small end temperature difference can occur in the recuperators. To explain this phenomenon, values of the end temperature differences of RHX1 and RHX2 are portrayed in Fig. 7.

The decrease of the recuperator end temperature difference is considerable at the hot end of the RHX2 at night. The value is less than 2°C. Such a small value of the end temperature difference is not desired. To protect this, some design change should be examined.

In addition, no consideration has been conducted for the turbomachinery design in this paper. However, the capacity of the solar power plant is rather small and aerodynamic designs of the compressors are not easy due to the combination of a high pressure ratio and a small volume flow. Besides, there is a possibility of operation difficulty for the large pressure or temperature reductions from the rated values in the partial load operation. Further comprehensive studies are needed to clarify these problems.

These problems are derived from an extremely small power demand at midnight. Then, it will be considered that the aluminum volume is expanded to increase the energy storage capacity and small amount of surplus power will be generated and stored in the battery at midnight to flatten the power to adjust the demand.

## ENERGY BALANCE OF THE PLANT

Energy balance of the system is shown in Fig. 8. The total solar energy supplied to the receiver is 125 MW × 9 hr = 1125 MWhr. By deducting the reflection, radiation loss and convection loss, the thermal energy transferred to Na is 83.94MW and then, 83.94 MW x 9 hr = 755 MW.hr per day. By this thermal energy, electric power of 153.9 MWe.hr and 149.2 MWe.hr are produced at daytime and at night, respectively. Total electric power production is 303.1 MWe.hr per day.

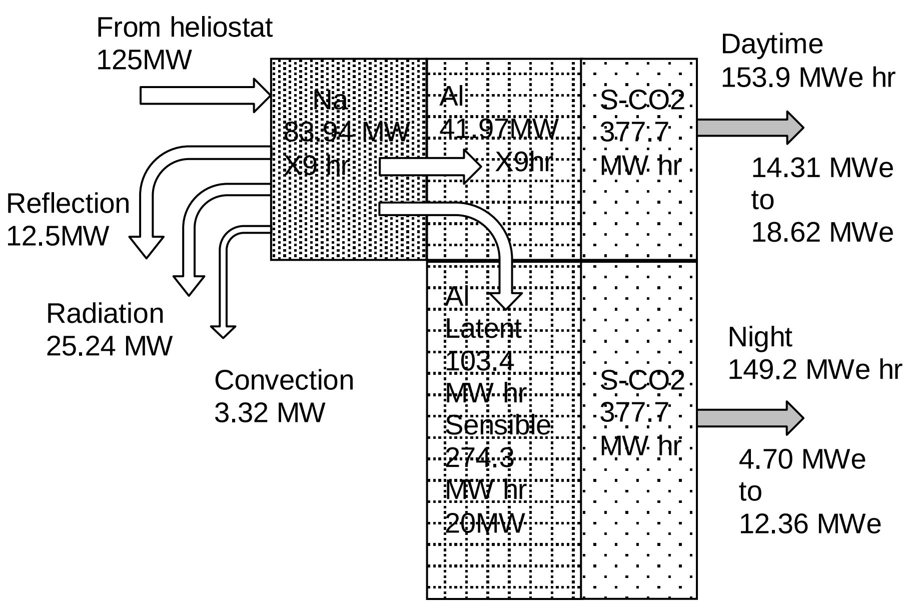


**Fig. 8. Total energy balance of the solar thermal power plant with Na cooled receiver, aluminum heat storage and S-CO2 GT.**

Therefore, the average cycle thermal efficiency becomes 40.1%.

The ratio of 303.1MWe.hr versus 1125 MW.hr means average thermal efficiency, which is 26.9%. This efficiency value doesn't include house load such as an operation power for the heliostats, Na and $CO_2$ pumping powers, cooling water pumping power and other miscellaneous powers. In the literature (Zhang, 2013), a value of 18.1% is reported as the mean gross efficiency as % of direct radiation in the existing solar power plant. Therefore, the above value of 26.9% seems fairly good, though several percentages must be deducted for the house loads.

The ratio of 303.1 MWe.hr versus 755.46 MW.hr means the value of the average cycle power generation efficiency, which is 40.12%. At midnight, the value of the cycle power generation efficiency is considerably reduced from the rated value of 47.26%. Taking this into consideration, the average value is not so low. In the steam turbine cycle, the complicated system including multi-stage steam extractions and the reheat turbine is needed to achieve efficiency of 40%. Therefore, the application of S-$CO_2$ –GT cycle is useful to the solar power system.

## CONCLUSION

For a 125 MW capacity solar plant, partial load calculations were conducted for a solar power system with a Na-cooled concentrated receiver, a Na-Al-$CO_2$ heat exchanger, and a supercritical $CO_2$ gas turbine. The flow scheme of S-$CO_2$ GT is one intercooled cycle with a bypass circuit. The rated turbine inlet pressure and temperature are, respectively, 20 MPa and 650°C. The recuperator design was produced based on a PCHE heat exchanger. The quasi-static calculations are based on several simplified assumptions. As results of calculations, time histories of the $CO_2$ pressure, temperature, generator power and the cycle thermal efficiency are obtained for the partial load operation through daytime and nighttime. The respective reductions of both values of the turbine inlet pressure and the turbine inlet temperature reached 9.1 MPa and 370°C. The low values lead to severe operation difficulties at the recuperator end temperature difference and some design improvement will be needed. The performances of compressors are not examined. The total thermal efficiency was calculated as reaching 26.9%, which is regarded as fairly good. Though more comprehensive research works are needed, it was decided that the day and night through operation of the new solar power system with the Na cooled receiver, aluminum heat storage and S-$CO_2$-GT is feasible.

## REFERENCES


Zhang, H. L., Baeyens, J., Degreve, J. and Caceres, G., 2013, “Concentrated solar power plants: Review and design methodology,” Renewable and Sustainable Energy Reviews, 22, 466-481.

Dunn, R. I. Hearps, P. J. and Wright, M.N., 2012, “Molten-salt power towers: Newly commercial concentrating solar storage,” Proceedings of the IEEE, 100(2), 504-515.

Hasuike, H., Yoshizawa, Y., Suzuki, A., Tamaura, Y., 2006, “Study on design of molten salt solar receivers for beam-down solar concentrator,” Solar Energy, 80, 1255-1262.

Muto, Y., Kato, Y., 2013, “Cycle Thermal Efficiency of Supercritical $CO_2$ Gas Turbine Dependent on Recuperator Performance,” Journal of Power and Energy Systems, 7(3) 1-14.

Muto, Y., Aritomi, M., Ishizuka, T., Watanabe, N., 2014, “Comparison of supercritical $CO_2$ gas turbine cycle and Brayton $CO_2$ gas turbine cycle for solar thermal power plants,” *Proc. of Fourth International Symposium – Supercritical $CO_2$ Power Cycles*, Pittsburgh, USA, September 9–10.

Muto, Y., Watanabe, N., Aritomi, M. Ishizuka, T., 2016, “Dependence of thermal efficiency on receiver temperature of solar thermal power systems combined with supercritical $CO_2$ gas turbine cycle and Brayton $CO_2$ gas turbine cycle,” *Proc. of Fifth International Symposium – Supercritical $CO_2$ Power Cycles*, San Antonio, USA, March 29–31.